# Micromechanical Modeling of Steady-State Deformation in Asphalt

V. S. Deshpande[1] and D. Cebon[2]

**Abstract:** A micromechanical model for the steady-state deformation of idealized asphalt mixes is presented. Triaxial compression tests were conducted on idealized asphalt mixes and the volumetric and deviatoric strains were measured. The specimens were observed to dilate under compressive stresses and the deformation behavior was seen to be dependent on the hydrostatic as well as the deviatoric stresses. A simple model for the nonlinear viscous steady-state behavior of idealized mixes is presented based on a ''shear box'' analogy. Predictions of the model are seen to agree well with experimental measurements for a wide range of conditions. An upper bound is calculated for the steady-state deformation rates within a plane strain half space comprising the idealized asphalt mix subject to a uniform pressure over a finite contact strip. The deformation rate varies nonlinearly with the applied load and is strongly dependent on the hydrostatic stress. Further, the deformation rate is seen to be a maximum at a position about half a contact length below the surface of the half space. These findings are in general agreement with wheel tracking experiments on these idealized mixes.

**DOI:** 10.1061/(ASCE)0899-1561(2004)16:2(100)

**CE Database subject headings:** Asphalt; Dilatancy; Micromechanics; Deformation; Models.

## Introduction

The development of a model for the rutting of flexible pavements relies, at least in part, on understanding the constitutive behavior of asphalt or bituminous mixes which are used in the upper layers of pavements. Bituminous mixes are complex multiphase materials consisting of a gradation of aggregate, air voids, and bitumen. Constitutive modeling of the deformation behavior of bituminous mixes using continuum *mechanics* has been the focus of research among paving technologists for over 50 years. In the past, most of these approaches have been empirical: The structure, applicability, and limitations of various existing models are discussed in Deshpande (1997). Here we briefly describe a few relevant micromechanical models.

To the writers' knowledge the first micromechanically motivated model was proposed by van der Poel (1958) based on the Fröhlich and Sack (1946) analysis of the effective moduli of a concentrated suspension of rigid spheres in an elastic matrix. Good agreement with experimental measurements of the dynamic stiffness (elastic) was observed for bituminous mixes with an aggregate volume fraction up to 60%.

Hills (1973) developed a creep model for asphalt with microstructural variables such as bitumen film thickness between aggregate particles as input variables. The imposed macroscopic strain on the bituminous mix was assumed to be accommodated on the microscopic scale by displacements of adjacent aggregate particles in both shear and compression. Employing this assumption, Hills calculated the effective elastic stiffness of the bituminous mix. The model provides a form for the constitutive equations but depends entirely on curve fitting to experimental data to obtain quantitative information.

In the spirit of the Hills' model, Cheung et al. (1999) used the isolated contact modeling approach originally developed for the analysis of Stage I powder compaction to rigorously analyze the deformation behavior of an asphalt idealized as a random distribution of rigid spheres separated by thin films of bitumen. The predictions of the model agree qualitatively with experimental measurements but the isolated contact model substantially underpredicts the ''stiffening'' effect of the aggregate.

All the above models provide closed form relations for the deformation response of asphalt. Discrete element simulations have also been employed to gain insight into the fundamental mechanisms of the deformation of asphalt; see for example Rothenburg et al. (1992). In these models the bituminous mix is represented by a set of discrete elastic particles separated by a visco-elastic binder. Computational time constraints dictate that such models can rarely be used to simulate deformation in a pavement.

This paper presents a micromechanical model of the deformation of asphalt that gives a simple analytical constitutive relation in terms of measurable mix parameters like volume fractions of voids and aggregate. The basic approach is very general and involves a methodology for combining the measured behavior of the bitumen with some simple assumptions about the behavior of the aggregate to give a constitutive relation for the bituminous mix. Here for simplicity the model is presented for the steady-state nonlinear viscous behavior of bitumen but the approach can easily be extended to a more complicated and complete visco-elastic model for the bitumen.

[1]Engineering Dept., Cambridge Univ., Trumpington St., Cambridge CB2 1PZ, UK.

[2]Engineering Dept., Cambridge Univ., Trumpington St., Cambridge CB2 1PZ, UK (corresponding author). E-mail: dc@eng.cam.ac.uk

Note. Associate Editor: Louay N. Mohammad. Discussion open until September 1, 2004. Separate discussions must be submitted for individual papers. To extend the closing date by one month, a written request must be filed with the ASCE Managing Editor. The manuscript for this paper was submitted for review and possible publication on May 8, 2002; approved on April 29, 2003. This paper is part of the ***Journal of Materials in Civil Engineering***, Vol. 16, No. 2, April 1, 2004. ©ASCE, ISSN 0899-1561/2004/2-100–106/$18.00.

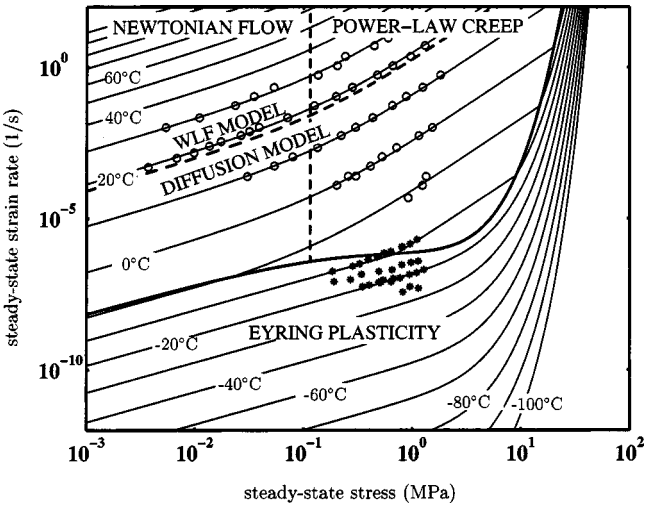


**Fig. 1.** Deformation mechanism map for steady-state behavior of 50 pen bitumen in tension (Cheung and Cebon 1997)

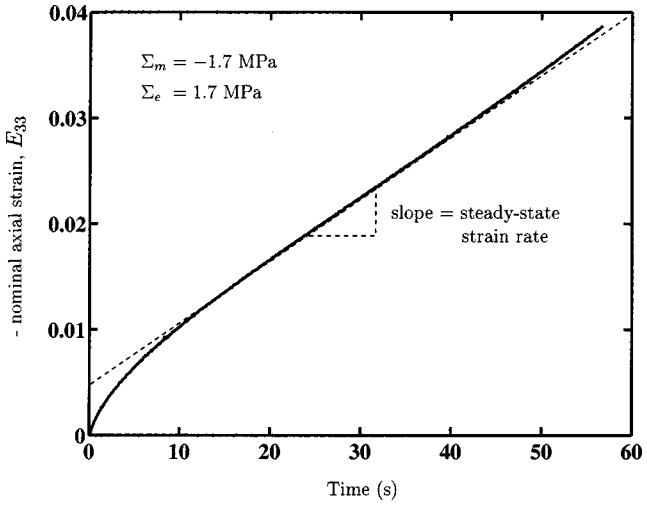


**Fig. 2.** Creep curve showing variation of axial strain $E_{33}$ versus time, from triaxial test on 64% idealized asphalt mix with $\eta=1.0$

## Steady-State Triaxial Behavior of Idealized Asphalt

Triaxial experiments on idealized asphalt are first detailed in this section. Insight gained into the deformation mechanisms from these experiments is then used to motivate a micromechanical model for the steady-state deformation of asphalt.

### *Steady-State Behavior of Pure Bitumen*

In order to develop a micromechanical model for the deformation of asphalt which is comprised of bitumen and aggregate, the behavior of pure bitumen was first characterized. Cheung and Cebon (1997) developed phenomenological models for the deformation behavior of a 50 pen (penetration grade of the bitumen) bitumen over a wide range of temperatures and strain rates (Anon 1989). The relationship between the steady-state stress and strain rate for the bitumen they tested in uniaxial tension is shown in Fig. 1 in the form of a ''deformation mechanism map.'' The map reveals a range of deformation mechanisms characterized by power-law and linear viscous relationships at high strain rates and Eyring plasticity at very low strain rates. The temperature dependence of the bitumen is diffusion controlled below approximately 20°C and Williams–Landel–Ferry (WLF) (Williams et al. 1955) governed at higher temperatures.

In this study we focus on the behavior of an idealized asphalt at 20°C. At this temperature the behavior of the 50 pen bitumen can be approximated as linear viscous below 0.1 MPa and power-law viscous at higher stress levels. Cheung and Cebon (1997) extended this uniaxial study to the multiaxial case by conducting shear experiments on thin annular rings of bitumen. These experiments indicated that the steady-state behavior of the pure bitumen is insensitive to the hydrostatic stress and thus a von Mises relation of the form

$$\frac{\dot{E}_{ij}}{\dot{\epsilon}_o}=\frac{3}{2}\left(\frac{\Sigma_e}{\sigma_o}\right)^{n-1}\frac{\Sigma'_{ij}}{\sigma_o} \tag{1}$$

is suitable to describe the steady-state multiaxial response of the pure bitumen. Here $\sigma_o$ and $\dot{\epsilon}_o$ are a reference stress and strain rate, respectively; while $\Sigma'_{ij}$=applied deviatoric stress; $\Sigma_e$=von Mises effective stress=$\sqrt{\frac{3}{2}\Sigma'_{ij}\Sigma'_{ij}}$; and $\dot{E}_{ij}$=steady-state strain rate. The creep exponent $n\approx 2.3$ in the power-law regime of behavior for the 50 pen bitumen tested by Cheung and Cebon (1997).

### *Steady-State Triaxial Behavior of Idealized Asphalt*

Cylindrical specimens of an idealized asphalt comprising 64% by volume sand particles graded between 300 and 600 μm and 4% by volume air voids were manufactured using the bitumen described above (see Deshpande and Cebon 2000 for details of the manufacturing process). Axisymmetric stress path tests were conducted in a standard soil-mechanics triaxial test cell with the axial stress $\Sigma_{33}$ applied by a hydraulic testing machine and the radial stress $\Sigma_{11}=\Sigma_{22}$ applied via a pressuring fluid (water). The hydrostatic and von Mises effective stresses defined by

$$\Sigma_m=\frac{\Sigma_{33}+2\Sigma_{11}}{3} \tag{2a}$$

and

$$\Sigma_e=|\Sigma_{33}-\Sigma_{11}| \tag{2b}$$

respectively, can be varied independently in this setup. Proportional loading stress path tests were conducted for a number of stress paths defined by $\Sigma_m=-\eta\Sigma_e$, with the value of the parameter $\eta$ taking values in the range $\eta=1/3$ (for uniaxial compression) to $\eta=1.0$. At each value of the stress ratio $\eta$ the effective stress $\Sigma_e$ was varied by over 3 orders of magnitude in order to investigate the strain rate sensitivity of the idealized asphalt.

A typical triaxial creep test on the idealized asphalt is shown in Fig. 2 for a stress ratio $\eta=1.0$ and applied effective stress $\Sigma_e=1.7$ MPa. The creep curve, which is a plot of the axial strain $E_{33}$ versus time, can be divided into three regions: Primary creep ($-E_{33}<0.01$) where the strain rate decreases with time; secondary creep ($0.01<-E_{33}<0.025$) where the strain rate remains constant; and tertiary creep ($-E_{33}>0.025$) where the strain rate increases. The steady-state creep response of the material is defined as the secondary creep strain rate.

The steady-state axial creep behavior observed from triaxial tests on the idealized asphalt at 20°C is summarized in Fig. 3 where the steady-state axial strain rate is plotted against the applied effective stress $\Sigma_e$. Also shown in Fig. 3 is the curve rep-

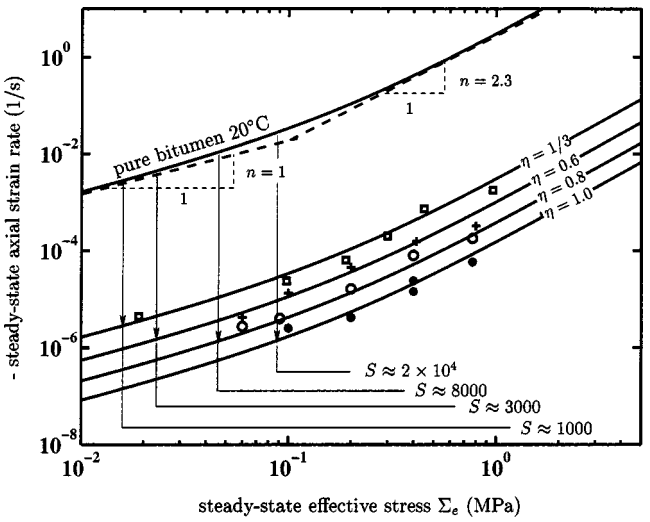


**Fig. 3.** Steady-state deformation behavior of 64% idealized asphalt mix at 20°C under various triaxial stress states

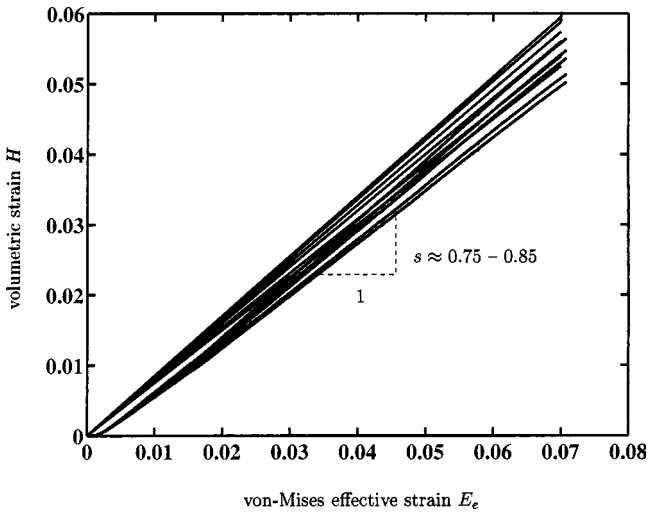


**Fig. 4.** Variation of volumetric strain $H$ with von Mises effective strain $E_e$ for triaxial tests on 64% idealized asphalt mix. Data are plotted for all tests conducted.

resenting the uniaxial steady-state behavior of bitumen at 20°C (from Fig. 1). Since the deformation behavior of bitumen is independent of the hydrostatic stress [see Eq. (1)] this curve is the same for all stress states. A comparison of the steady-state behavior of the bitumen and idealized asphalt shown in Fig. 3 reveals that for a given stress ratio $\eta$, the form of the steady-state stress versus strain rate relationship of the idealized asphalt and bitumen are similar and can be described by modifying Eq. (1) (the power-law creep equation employed for characterizing the bitumen) simply as

$$\frac{\dot{E}_{ij}}{\dot{\epsilon}_o} = \frac{3}{2}\left(\frac{\Sigma_e}{\sigma_o}\right)^{n-1}\frac{\Sigma'_{ij}}{S\sigma_o} \tag{3}$$

Here the ''stiffening'' factor $S$ is defined as the ratio of the steady-state deformation rate of the bitumen to the steady-state deformation rate of the mix subjected to the same effective stress $\Sigma_e$. $S$ is a function of the stress ratio $\eta$ and it varies from $S \approx 1000$ for uniaxial compression ($\eta = 1/3$) to $S \approx 2 \times 10^4$ for $\eta = 1.0$. It is worth noting that the mix exhibits linear viscous behavior [Eq. (3) with $n = 1$] for $\Sigma_e < 0.1$ MPa and power-law behavior [Eq. (3) with $n = 2.3$] at higher stresses. Thus, the transition from linear to power-law behavior occurs at approximately 0.1 MPa for both pure bitumen and the mix.

The stress ratio dependence of the deformation of the idealized asphalt suggests that unlike pure bitumen the asphalt does not undergo incompressible deformation. The volumetric strain

$$H = E_{33} + 2E_{11} \tag{4}$$

is plotted as a function of the von Mises effective strain

$$E_e = \tfrac{2}{3}|E_{33} - E_{11}| \tag{5}$$

in Fig. 4, for the triaxial tests conducted on the idealized asphalt over a wide range of temperatures and strain rates. To within experimental error, the relation between $H$ and $E_e$ can be seen to be simply represented by

$$H = sE_e \tag{6}$$

where $s$=dilation gradient ($s \approx 0.75 - 0.85$). This implies that the dilational behavior is a result of the kinematic constraint imposed by the aggregate ''skeleton'' and is not dependent on the properties of the bitumen. Note that the usual sign convention that a positive $H$ corresponds to a volume increase or dilation is employed in Eq. (6).

### Steady-State Constitutive Relation for Idealized Asphalt

The dilational behavior observed in the idealized asphalt is analogous to the behavior of some soils. In this section a micromechanical model for asphalt based on this analogy is briefly described. Readers are referred to Deshpande and Cebon (1999a) for details of this analysis.

Consider a shear-box test on close-packed rigid spheres as shown in Fig. 5. As the relative shear displacement of the two halves of the shear box is increased by $dx$ the two halves separate by an amount $dy$ due to the kinematic constraints imposed by the rigid spheres: the spheres can shear relative to each other only by riding up on each other. The quantity $dy/dx$ indicates the dilation in the shear zone. In most soils, at large strains, a slip zone develops and shear straining can occur without further dilation as sketched in Fig. 5(b). A thin layer of soil in the slip zone is then

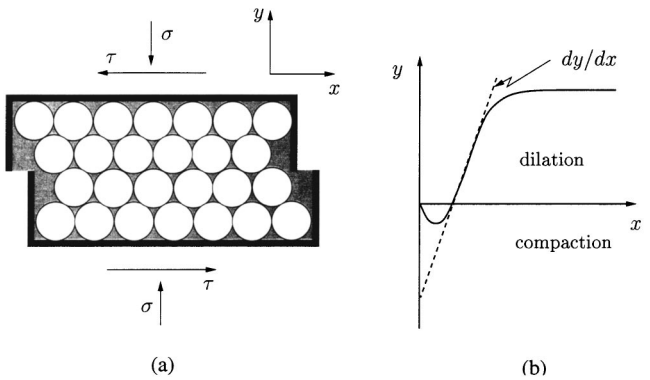


**Fig. 5.** Shear box analogy: (a) direct shear box test of granular materials and (b) variation of normal displacement $y$ with shear displacement $x$

said to have reached its critical state. A work equation for the shear box test on a dry soil can be written as

$$\tau\, dx - \sigma\, dy = \mu\sigma\, dx \tag{7}$$

where $\mu\, dx$ represents the frictional dissipation and $-\sigma\, dy$=work done against dilation (here a compressive $\sigma$ is taken as positive in line with the usual soil mechanics convention). The idealized asphalt comprises a dense packing of rigid particles with bitumen filling the gaps between the particles. Assuming no frictional contact between the particles (i.e., full lubrication of the particles by the bitumen) a work equation for the idealized asphalt, analogous to the shear box test equation for soils, with the frictional dissipation replaced by the viscous dissipation is given by

$$\Sigma_m \dot{H} + \Sigma_e \dot{E}_e = \dot{D} \tag{8}$$

Here $\Sigma_m \dot{H}\,(\equiv\sigma\, dy)$ represents the volumetric work; $\Sigma_e \dot{E}_e$ $(\equiv\tau\, dx)$=shear or ''shape'' work; and $\dot{D}$=viscous dissipation rate.

It now remains to specify the viscous dissipation rate. The idealized asphalt is a particulate composite comprising rigid inclusions and voids in a power-law viscous matrix. The dissipation rate in the matrix is estimated by employing the Hashin ''composite sphere'' model (Hashin 1962) for a linear viscous composite and then transforming to the power-law viscous case using an upper bound transformation proposed by Suquet (1993); see details in Deshpande and Cebon (1999b) including a discussion on the stiffening as a function of the volume fraction of aggregate. For an idealized asphalt comprising volume fractions $c$ of rigid inclusions and volume fraction $v$ of voids, the dissipation rate $\dot{D}$ is given by

$$\dot{D} \leqslant \frac{\sigma_o}{\dot{\epsilon}_o^{1/n}} \left( \frac{1}{2} k \dot{H}^2 + \frac{3}{2} \mu \dot{E}_e^2 \right)^{(n+1)/2n} [1-(c+v)]^{(n-1)/2n} \tag{9a}$$

where

$$\mu = \frac{2}{3} \left[ 1 + \frac{c}{\frac{2}{5}(1-c) - \frac{c(1-c^{2/3})^2}{-\frac{10}{21}c^{7/3} + \frac{10}{21}}} - \frac{v}{\frac{3}{5} + \frac{2}{5}v + \frac{v(1-v^{2/3})^2}{\frac{95}{168}v^{7/3} + \frac{10}{21}}} \right] \tag{9b}$$

and

$$k = \frac{8}{9} \frac{1-v}{v} \frac{1}{1-c} \tag{9c}$$

The triaxial experiments indicated that the aggregate skeleton constrained the volumetric and von Mises strains via Eq. (6). Substituting Eq. (9*a*) into Eq. (8) and eliminating $H$ with Eq. (6) we obtain a constitutive relation for the steady-state behavior of the idealized asphalt as

$$\dot{E}_e \geqslant \frac{\dot{\epsilon}_o [1-s\eta]^n}{(\frac{1}{2}ks^2 + \frac{3}{2}\mu)^{(n+1)/2} [1-(c+v)]^{(n-1)/2}} \left( \frac{\Sigma_e}{\sigma_o} \right)^n \tag{10}$$

with the volumetric strain rate given by the time derivative of Eq. (6).

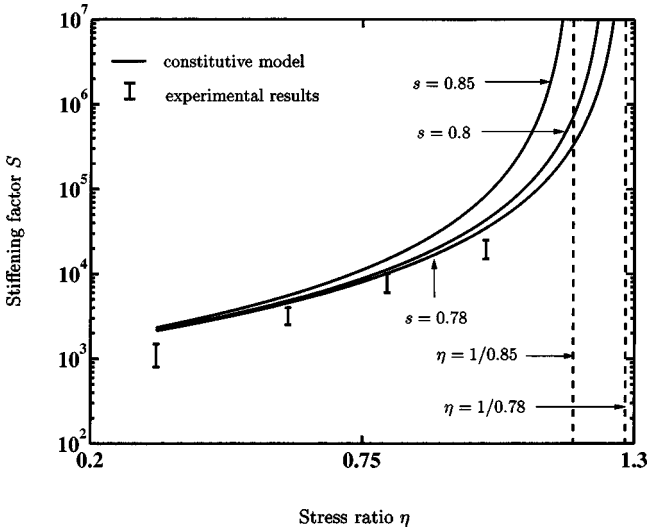


**Fig. 6.** Stiffening factor $S$ of 64% idealized asphalt mix as function of stress ratio $\eta$, for selected values of dilation gradient $s$. Experimental results (with associated uncertainty) are also shown.

To compare the predictions of this model with the experiments described above this general constitutive relation is rewritten for axisymmetric stress states. Substituting Eq. (10) into Eq. (5) and simplifying using Eq. (6) gives the axial and radial strain rates as

$$\dot{E}_{33} = \frac{\dot{\epsilon}_o}{S} \left( \frac{\Sigma_e}{\sigma_o} \right)^n \text{sign}(\Sigma) \tag{11a}$$

and

$$\dot{E}_{11} = \left( \frac{2s\ \text{sign}(\Sigma) - 3}{2s\ \text{sign}(\Sigma) + 6} \right) \dot{E}_{33} \tag{11b}$$

respectively, with the stiffening factor $S$ defined by

$$S = \frac{(\frac{1}{2}ks^2 + \frac{3}{2}\mu)^{(n+1)/2} [1-(c+v)]^{(n-1)/2}}{[1-s\eta]^n \left[ 1 + \frac{s\ \text{sign}(\Sigma)}{3} \right]} \tag{12}$$

Here $\Sigma = \Sigma_{33} - \Sigma_{11}$ is a measure of the deviatoric stress. Thus, we see that the predicted behavior has the same form as the experimental data with the stiffening factor a function of the volume fraction of the aggregate and voids and the stress ratio $\eta$.

The predicted dependence of the stiffening factor $S$ on the stress ratio $\eta$ for the idealized asphalt with 64% by volume sand is shown in Fig. 6 for three values of the dilation gradient $s$ (to account for the scatter seen in the experimental measurements plotted in Fig. 4). The experimental results plotted with error bars in Fig. 6 agree well with the model for $s=0.78$: this value of $s$ is within the range of experimentally measured values of $s$ indicating that the model fits the data well. Similarly, the model was seen to accurately predict the triaxial experimental results for tests on idealized asphalt mixes with 75% by volume sand (Deshpande and Cebon 1999a). It is worth noting that the model predicts ''lockup'' of the aggregate with no deformation for any applied deviatoric stress for a stress ratio $\eta = 1/s$. This critical value of $\eta$, shown by the dashed lines in Fig. 6, represents the asymptotes to the model.

## Deformation Behavior of Half-Space of Idealized Asphalt

Numerous researchers (e.g., Brown et al. 1980; Monismith et al. 1988; Collop et al. 1995) have evaluated the deformation of a

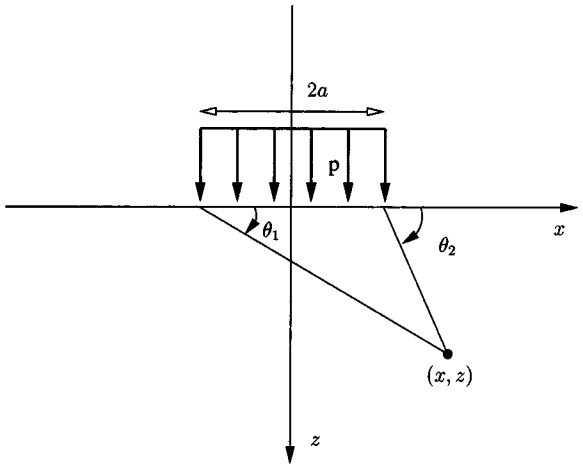


**Fig. 7.** Plane strain half-space model with uniform pressure loading over strip of width $2a$

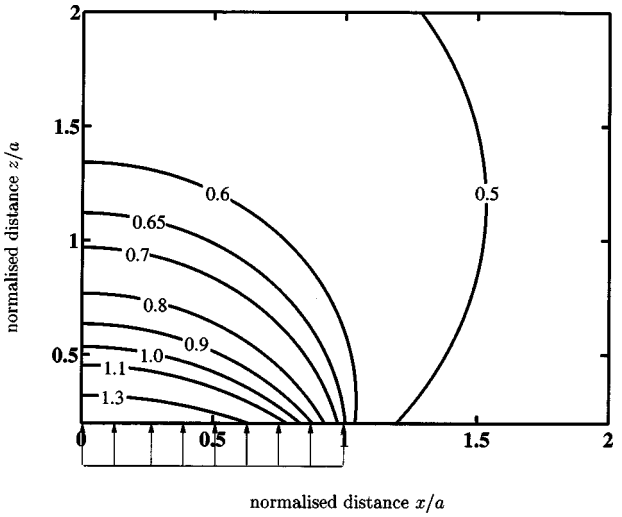


**Fig. 8.** Contours of stress ratio $\eta$ in plane strain elastic half space with Poisson's ratio $\nu=0.25$

bituminous pavement by modeling it as a linear viscoelastic layered half space. While these approaches capture the linear rate dependence of the above constitutive model they ignore the dependence on the stress ratio $\eta$ and the nonlinear rate sensitivity of the deformation behavior of asphalt. These factors were seen to be important in wheel tracking tests conducted by Collop and Khanzada (2001) on idealized asphalt mixes.

There are no known analytical results for the behavior of a half space of a material with constitutive relation (10). Finite element calculations with this new constitutive relation will need to be performed in order to obtain exact numerical solutions. To explore the effect of the dilatancy of the asphalt, an upper bound solution is developed here for the deformation rate within a plane strain half space subjected to a uniform pressure loading $p$ over a strip $(-a\leqslant x\leqslant a)$ as shown in Fig. 7.

The stresses at a general point in a plane strain elastic half space due to uniform normal pressure $p$ over a strip of width $2a$ are given by Johnson (1985) as

$$\sigma_{xx}=-\frac{p}{2\pi}[2(\theta_1-\theta_2)-(\sin 2\theta_1-\sin 2\theta_2)] \tag{13a}$$

$$\sigma_{zz}=-\frac{p}{2\pi}[2(\theta_1-\theta_2)+(\sin 2\theta_1-\sin 2\theta_2)] \tag{13b}$$

$$\sigma_{yy}=\nu(\sigma_{xx}+\sigma_{zz}) \tag{13c}$$

$$\sigma_{xz}=-\frac{p}{2\pi}[\cos 2\theta_1-\cos 2\theta_2] \tag{13d}$$

where $\theta_1$ and $\theta_2$ are defined in Fig. 7 and $\nu$=Poisson's elastic ratio. The hydrostatic stress $\Sigma_m$ and von Mises effective stress $\Sigma_e$ are then given by

$$\Sigma_m=\frac{\sigma_{xx}+\sigma_{yy}+\sigma_{zz}}{3} \tag{14a}$$

and

$$\Sigma_e=\sqrt{\frac{3}{2}[(\sigma_{xx}-\Sigma_m)^2+(\sigma_{yy}-\Sigma_m)^2+(\sigma_{zz}-\Sigma_m)^2+2\sigma_{xz}^2]}, \tag{14b}$$

respectively. Contours of the stress ratio $\eta=-\Sigma_m/\Sigma_e$ with $\nu=0.25$ are plotted in Fig. 8: Stress ratio $\eta$ is seen to be a maximum at the contact patch and decreases with distance from the contact region.

We proceed by employing the above stress distribution to estimate the deformation rates pointwise in the half space through the constitutive relation (10). This stress field satisfies equilibrium but by using the constitutive relation pointwise to estimate the deformation rate we neglect compatibility of the velocity fields. This implies that the method will give an upper bound on the deformation rate (i.e., the actual deformation rate will be lower) since the constraints imposed by the surrounding material are neglected. It is worth mentioning here that the above prescription gives a rigorous upper bound on the deformation rate for a stable material (Drucker 1953): neglecting the effects of cracking the idealized asphalt exhibits stable behavior (see Lubliner 1990 for a discussion on extremum principles).

The constitutive relation (10) specifies the von Mises effective strain rate for an applied stress state. Noting that the effective stress at any point in the half space is directly proportional to the applied pressure $p$, a normalized effective strain rate $\hat{\dot{E}}_e$ can be written as

$$\hat{\dot{E}}_e=\frac{\dot{E}_e}{\dot{\epsilon}_o}\left(\frac{\sigma_o}{p}\right)^n\left(\frac{1}{2}ks^2+\frac{3}{2}\mu\right)^{(n+1)/2}[1-(c+v)]^{(n-1)/2}$$
$$=(1-\eta s)^n\left(\frac{\Sigma_e}{p}\right)^n \tag{15}$$

This normalized strain rate $\hat{\dot{E}}_e$ is plotted in Fig. 9 with $s=0.78$, as a function of horizontal distance $x$ for various depths $z$ below the surface of the half space. Interestingly, the deformation rate is seen to increase with depth initially and then decrease. Contours of constant $\hat{\dot{E}}_e$ are plotted in Fig. 10. The shaded region in Fig. 10 corresponds to a zone of the maximum deformation rate: it is approximately a semicircle at a radius $R\approx a$. At radii $R\gg a$ the effective stress is too small to cause flow, while at $R\ll a$ the high value of the stress ratio $\eta$ means that the idealized asphalt mix has ''locked up'' with deformation severely restricted. These findings are in qualitative agreement with the experimental observations of Collop and Khanzada (2001).

In the analysis described above, the stress state was calculated with an assumed elastic Poisson's ratio $\nu=0.25$. A series of cal-

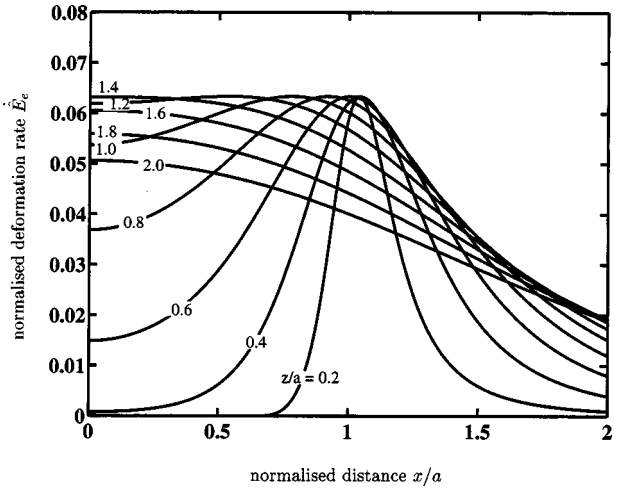


**Fig. 9.** Normalized deformation rate $\hat{\dot{E}}_e$ in plane strain half space of 64% idealized mix with $s=0.78$

culations with other values of $\nu$ were performed but no qualitative changes in the results were seen with the deformation rate always being a maximum in a semicircular zone at a radius $R \approx a$. Thus, we conclude that a half space of a material made from the dilatant asphalt characterized by the constitutive relation (10) is expected to undergo the most severe deformation below the surface. This is similar to contact problems in metal plasticity (Johnson 1985).

## Discussion

In the constitutive model developed here, asphalt was modeled as a multiphase composite comprising rigid aggregate, pure bitumen, and voids. The constitutive properties of the bitumen are taken as an input into the model and the bitumen assumed to be nonlinear viscous. These properties of the bitumen can be modified to say that of mastic (bitumen plus filler) using the model derived in Deshpande (1997). Similarly some aggregate properties are also taken as experimental inputs into the constitutive model. In particular, the high volume fraction of rigid aggregate forms a structural skeleton which imposes kinematic constraints on the deformation, i.e., shear deformation is accompanied by dilation. The aggregate properties, like the particle shapes and gradation of sizes, control the exact relation between the shear and dilational strains. No effort is made to model this complex phenomena in the model. Instead, the experimentally measured dilation gradient is taken as an input to the model.

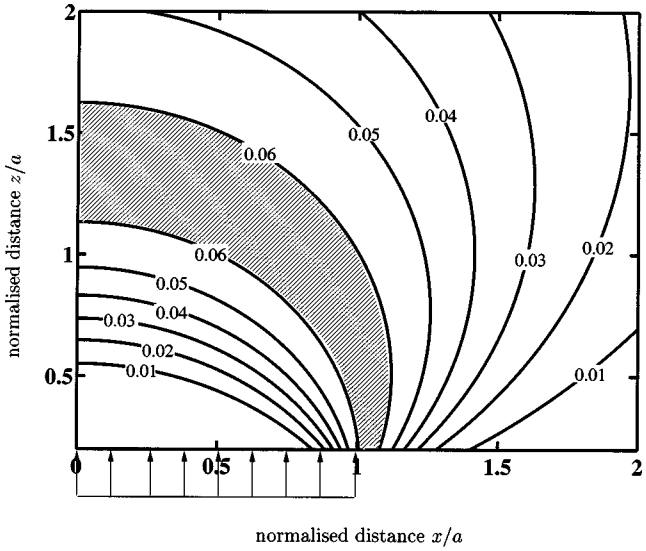


**Fig. 10.** Contours of normalized deformation rate $\hat{\dot{E}}_e$ in half space of 64% idealized mix

The steady-state constitutive model presented here is shown to agree well with the experimentally measured steady-state response of idealized asphalt mixes over a wide range of stress states and strain rates. However, there are two main limitations of the model in the current form: (1) The model assumes only steady-state behavior with all deformation assumed to be permanent and (2) all the dissipation is assumed to be viscous with any interparticle contact assumed to give rise only to the kinematic constraint which results in dilation, i.e., frictional dissipation is neglected. Given these limitations it is worth noting that the model has been used successfully to predict the uniaxial steady-state deformation behavior of an asphalt mix with 85% by volume of aggregate which was cored from a compacted slab (Deshpande and Cebon 2000). However, while the steady-state model has limited applicability for simulating realistic asphalt behavior under wheel loads, the theoretical framework presented here is extendible and more realistic aggregate and bitumen properties (e.g., a viscoelastic model for the bitumen) can be employed with appropriate modifications to the dissipation relation (9*a*).

## Concluding Remarks

A micromechanical model which characterizes the steady-state, nonlinear viscous behavior of an idealized asphalt was presented. Analogous to some soil mechanics models it is argued that viscous dissipation and particle interlocking contribute to the strength of the asphalt: at lower triaxialities the viscous term dominates, but with increasing hydrostatic pressure the strength of the mix rises dramatically until ''lockup'' is achieved. In the micromechanical model presented the viscous dissipation was estimated from a nonlinear composite theory in terms of the volume fraction of the aggregate and voids. The interlocking term was estimated from the measured dilation of the idealized asphalt mixes. Good agreement between the model and triaxial experiments on an idealized asphalt mix was seen over a wide range of stress states and strain rates, with the only inputs to the model being the properties of the bitumen, volume fractions of the constituents, and the (measured) dilation gradient of the aggregate.

To gauge the implications of this dilatant constitutive relation, the deformation rates in a pavement were modeled approximately using a plane strain half-space analysis. The maximum deformation rate was seen to occur below the road surface and at a radius equal to about half the contact width of the loading strip.

This study represents a first step towards a more complete micromechanical model for asphalt. The framework presented here can be extended to the transient and cyclic behavior of asphalt which is more relevant to the rolling load situation in roads. These issues will be addressed in future studies.

## Acknowledgment

The writers are grateful to the Nottingham Asphalt Research Consortium (NARC) for their financial support.

## References


Anon. (1989). ''Bitumens for building and civil engineering. Part 1. Specification of bitumens for road purposes.'' *BS 3690*, British Standards Institution, London.

Brown, S. F., Stock, A. F., and Pell, P. S. (1980). ''The structural design of asphalt pavements by computer.'' *J. Inst. Highway Eng.*, 27(3), 2–10.

Cheung, C. Y., and Cebon, D. (1997). ''Experimental study of pure bitumen in tension, compression and shear.'' *J. Rheol.*, 41(1), 45–73.

Cheung, C. Y., Cocks, A. C. F., and Cebon, D. (1999). ''Isolated contact model for an idealized asphalt mix.'' *Int. J. Mech. Sci.*, 41, 767–792.

Collop, A. C., Cebon, D., and Hardy, M. S. A. (1995). ''Viscoelastic approach to rutting in flexible pavements.'' *J. Transp. Eng.*, 121(1), 82–93.

Collop, A. C., and Khanzada, S. (2001). ''Permanent deformation in idealized sand asphalt bituminous mixtures.'' *Int. J. Road Mater. Pavement Design*, 2(1), 7–28.

Deshpande, V. S. (1997). ''Steady-state deformation behavior of bituminous mixes.'' PhD thesis, Univ. of Cambridge, Cambridge, U.K.

Deshpande, V. S., and Cebon, D. (1999b). ''Models of particle reinforced nonlinear-viscous composite.'' *J. Eng. Mech.*, 125(3), 255–262.

Deshpande, V. S., and Cebon, D. (1999a). ''Steady-state constitutive relationship for idealized asphalt mixes.'' *Mech. Mater.*, 31(4), 271–287.

Deshpande, V. S., and Cebon, D. (2000). ''Uniaxial experiments on idealized asphalt mixes.'' *J. Mater. Civ. Eng.*, 12(3), 262–271.

Drucker, D. C. (1953). ''Coulomb friction, plasticity and limit loads.'' *J. Appl. Mech.*, 53, 57–65.

Fröhlich, H., and Sack, R. (1946). ''Theory of the rheological properties of dispersions.'' *Proc. R. Soc. London, Ser. A*, 185, 415–430.

Hashin, Z. (1962). ''The elastic moduli of heterogeneous materials.'' *J. Appl. Mech.*, 29, 143–150.

Hills, J. F. (1973). ''The creep of asphalt mixes.'' *J. Inst. Pet.*, 59(570), 247–262.

Johnson, K. L. (1985). *Contact mechanics*, Cambridge Univ. Press, Cambridge, U.K.

Lubliner, J. (1990). *Plasticity theory*, Maxwell Macmillan International, New York.

Monismith, C. L., Sousa, J., and Lysme, J. (1988). ''Modern pavement design technology including dynamic load conditions.'' *Proc., SAE Conf. on Vehicle/Pavement Interaction*, SAE, Indianapolis.

Rothenburg, L., Bogobowicz, A., Haas, R., Jung, F. W., and Kennepohl, G. (1992). ''Micromechanical modelling of asphalt concrete in connection with pavement rutting problems.'' *Proc., 7th Int. Conf. on the Structural Design of Asphalt Pavements*, Univ. of Michigan, Road Research Laboratory, Ann Arbor, Mich. 476–498.

Suquet, P. M. (1993). ''Overall potentials and extremal surfaces of power law or ideally plastic composites.'' *J. Mech. Phys. Solids*, 41(6), 981–1002.

van der Poel, C. (1958). ''On the rheology of concentrated suspensions.'' *Rheol. Acta*, 1, 198–205.

Williams, M. L., Landel, R. F., and Ferry, J. D. (1955). ''The temperature dependence of relaxation mechanisms in amorphous polymers and other glass-forming liquids.'' *J. Am. Chem. Soc.*, 77, 3701–3707.